Article

Interrogation of Surfaces for the Quantification of Adsorbed Species on Electrodes: Oxygen on Gold and Platinum in Neutral Media

Joaqui#n Rodri#guez-Lo#pez, Mario A. Alpuche-Avile#s, and Allen J. Bard

J. Am. Chem. Soc., **2008**, 130 (50), 16985-16995 • DOI: 10.1021/ja8050553 • Publication Date (Web): 21 November 2008

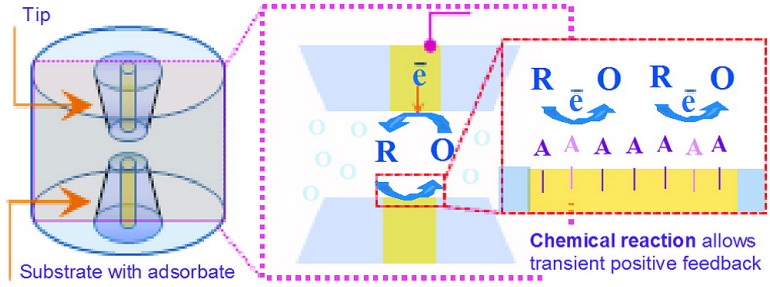

More About This Article

Additional resources and features associated with this article are available within the HTML version:

- Supporting Information
- Access to high resolution figures
- Links to articles and content related to this article
- Copyright permission to reproduce figures and/or text from this article

View the Full Text HTML

J|A|C|S
ARTICLES

Published on Web 11/21/2008

Interrogation of Surfaces for the Quantification of Adsorbed Species on Electrodes: Oxygen on Gold and Platinum in Neutral Media†

Joaquín Rodríguez-López, Mario A. Alpuche-Avilés, and Allen J. Bard*

Center for Electrochemistry, Department of Chemistry and Biochemistry, Center for Nano- and Molecular Science and Technology, The University of Texas at Austin, Austin, Texas 78712

Received July 10, 2008; E-mail: ajbard@mail.utexas.edu

Abstract: We introduce a new in situ electrochemical technique based on the scanning electrochemical microscope (SECM) operating in a transient feedback mode for the detection and direct quantification of adsorbed species on the surface of electrodes. A SECM tip generates a titrant from a reversible redox mediator that reacts chemically with an electrogenerated or chemically adsorbed species at a substrate of about the same size as the tip, which is positioned at a short distance from it (ca.1 μm). The reaction between the titrant and the adsorbate provides a transient positive feedback loop until the adsorbate is consumed completely. The sensing mechanism is provided by the contrast between positive and negative feedback, which allows a direct quantification of the charge neutralized at the substrate. The proposed technique allows quantification of the adsorbed species generated at the substrate at a given potential under open circuit conditions, a feature not attainable with conventional electrochemical methods. Moreover, the feedback mode allows the tip to be both the titrant generator and detector, simplifying notably the experimental setup. The surface interrogation technique we introduce was tested for the quantification of electrogenerated oxides (adsorbed oxygen species) on gold and platinum electrodes at neutral pH in phosphate and TRIS buffers and with two different mediator systems. Good agreement is found with cyclic voltammetry at the substrate and with previous results in the literature, but we also find evidence for the formation of "incipient oxides" which are not revealed by conventional voltammetry. The mode of operation of the technique is supported by digital simulations, which show good agreement with the experimental results.

Introduction

The electrochemical investigation of outer-sphere electron-transfer reactions coupled to complicated homogeneous reactions has become highly developed over the past decades because of the utilization of powerful techniques like cyclic voltammetry (CV), ultramicroelectrode (UME) voltammetry, and digital simulations.[1,2] However, understanding inner-sphere electrocatalytic reactions is more difficult because of their greater complexity and the difficulty in obtaining reliable quantitative data about intermediates and products on electrode surfaces. While a variety of electrochemical and surface spectroscopic methods that can be employed with electrodes in solution have been developed,[3] it has been difficult to obtain the needed versatility and sensitivity to address these kinds of reactions. We propose here an in situ electrochemical technique based on the scanning electrochemical microscope (SECM)[4] for the quantification of adsorbed species at electrodes that we hope will have an impact in this area. The operation of this technique is based on the feedback mode of SECM, which is one of the first developed[5] and perhaps one of the most distinctive of this electroanalytical tool. This is due to its ability to correlate an electrochemical signal at the SECM tip to topographical, chemical, and electrochemical features[6] in such distinct systems as the imaging of interdigitated arrays[7] or the components of a leaf,[8] the detection of an immobilized enzyme,[9] and the heterogeneous kinetics of semiconductors.[10] The SECM tip is able to detect changes in the electrochemical signal by the concurrent production and collection of the species of a mediator pair (O/R, where only one of the species is present initially in solution); variations in the diffusive flux of these species caused by interaction with the substrate allow the current measured at the SECM tip to respond accordingly. One of the most useful features of SECM is the ability to calculate the tip current as a function of different solution and interfacial phenomena, i.e.,

† This paper is no. 61 of the series Scanning Electrochemical Microscopy.

(1) Bard, A. J.; Faulkner, L. R. *Electrochemical Methods*; Wiley: New York, 2001.
(2) Saveant, J.-M. *Elements of Molecular and Biomolecular Electrochemistry*; Wiley-Interscience: Hoboken, NJ, 2006.
(3) *Electrochemical Interfaces. Modern Techniques for In-Situ Interface Characterization*; Abruña, H. D., Ed.; VCH: New York, 1991.
(4) *Scanning Electrochemical Microscopy*; Bard, A. J., Mirkin, M. V., Eds.; Marcel Dekker: New York, 2001.
(5) Bard, A. J.; Denuault, G.; Lee, C.; Mandler, D.; Wipf, D. O. *Acc. Chem. Res.* **1990**, *23*, 357–363.
(6) Bard, A. J.; Fan, F. F.; Pierce, D. T.; Unwin, P. R.; Wipf, D. O.; Zhou, F. *Science* **1991**, *254* (5028), 68–74.
(7) Wipf, D. O.; Bard, A. J. *Anal. Chem.* **1992**, *64*, 1362–1367.
(8) Lee, C.; Kwak, J.; Bard, A. J. *Proc. Natl. Acad. Sci. U.S.A.* **1990**, *87*, 1740–1743.
(9) Pierce, D. T.; Bard, A. J. *Anal. Chem.* **1993**, *65*, 3598–3604.
(10) Horrocks, B. R.; Mirkin, M. V.; Bard, A. J. *J. Phys. Chem.* **1994**, *98*, 9106–9114.

10.1021/ja8050553 CCC: $40.75

electrochemical kinetics, by digital simulation.[4] We can then consider the mediator pair to be an interrogation agent that reports to the SECM tip about the state of the surface being examined.

The technique proposed here consists of approaching a SECM tip to a small substrate, e.g., both 12.5 μm in radius, a, held at a short distance, d, from each other of ca. 1 μm ($L = d/a \leq 0.1$). The sensing mechanism is based on first bringing the substrate to a potential to generate an intermediate or product on the electrode surface and then taking the substrate to open circuit and allowing the tip-generated member of the redox pair to react chemically with an adsorbed species at the substrate electrode. The tip current during this last stage reports the amount of adsorbate to the SECM tip through a feedback loop. The chemical aspects of this application, in a sense, are analogous to modulated beam relaxation spectroscopy used in vacuum for gas−solid studies of catalysis,[11] as a generated reactive species is allowed to interact with an adsorbate. In another sense, however, it is a unique technique, as the reactive species generation and the detection scheme are integrated into the same electrochemical setup as enabled by the feedback mode of SECM and correspondingly intended for its use in solution. The SECM has been used previously for novel studies on a variety of surfaces and interfaces, such as in the quantification of intermediates released during an electrochemical reaction,[12,13] in the study of the kinetics of adsorption[14] and desorption[15] at pH-sensitive surfaces, and for the measurement of the steady-state kinetics at a catalytic substrate[16] or the binding of metal ions at lipid monolayers;[17] some studies have used a reactive mediator to measure binding kinetics[18] at self-assembled monolayers.

In this work we use transient SECM current measurements, which have been implemented in SECM before, e.g., chronoamperometry[19] and cyclic voltammetry.[20,21] The study of the effects of mediator surface diffusion,[15,22,23] applications to the study of lateral charge propagation in polymer films[24,25] and diffusion in monolayers,[26] and the detection of reactive species in living cells[27] have been developed through the use of this transient feedback mode. Some of these studies rely on the purposeful integration of a reactive species into the system; however, to the best of our knowledge, no SECM approach to the detection and quantification of transient reaction intermediates at electrocatalytic and catalytic materials (i.e., potential or nonpotential dependent) has been reported. This surface interrogation method allows the detection and quantification of only reactive adsorbed intermediates formed upon operation of the substrate electrode, independent of their spectroscopic characteristics and their electrochemical reactivity at the same substrate. We hope this technique will ultimately shed some light on inner-sphere mechanisms and be of use to a wider audience of surface chemists and electrochemists. We introduce the application of the technique with the quantification of gold and platinum oxides at neutral pH because they represent a classical example of the stable chemisorption of oxygen and formation of surface oxides.[28]

Mode of Operation

The technique takes advantage of the contrast obtained in the feedback operation mode of SECM. The SECM tip is a UME disk sealed in an insulating material. When the tip is biased to electrolyze a mediator at the diffusion-limited rate in the bulk solution, $i_{T,\infty}$, and approached to a substrate, the tip current becomes a function of the nature of the substrate and the tip−substrate distance, d. The distance normalized to the tip radius, a, or $L = d/a$, gives a convenient way to describe the steady-state current as a function of distance, i.e., an approach curve. A substantial change in the SECM tip current is observed when the distance between the tip and substrate is less than one radius of the tip, $L < 1$. Such changes in current are generally described in terms of dimensionless parameters like $I_T = i_T/i_{T,\infty}$, where i_T is the actual tip current and $i_{T,\infty}$ is the current far away from the substrate. At a given value of L, for positive feedback, $I_T > 1$ and for negative feedback $I_T < 1$, with intermediate regimes achieved by either changing conditions such as the substrate potential under kinetically limited conditions, decreasing the substrate size to a diameter of the order of the tip or during short transients.

Total positive feedback is obtained when a substrate regenerates the mediator at a rate limited only by diffusion in the tip−substrate gap. For example, for reduction at the tip ($O + e \rightarrow R$), the reaction at the substrate electrode would be the opposite electrochemical reaction ($R - e \rightarrow O$). While most SECM studies are done at steady state, in the experiments presented here, a transient chemical reaction of a species on the substrate is used to generate the positive feedback loop. Figure 1 illustrates the proposed mechanism for the surface interrogation of a reducible adsorbed species at the substrate. First, as depicted in Figure 1A, the substrate is pulsed or scanned to a potential where oxidation occurs and an adsorbed species, A, is formed; the tip at this time is kept at open circuit. The solution contains the mediator in its oxidized state, O, which is stable under these conditions and does not participate in any reaction. Following this, as shown in Figure 1B, the substrate electrode is taken to open circuit, and the tip is scanned or pulsed to reduce O and generate R. After R diffuses across the tip−substrate gap, it reaches the adsorbed species A and reacts chemically with it. O is regenerated and A is consumed and

(11) Asscher, M.; Somorjai, G. A. Reactive Scattering. In *Atomic and Molecular Beam Methods*; Scoles, G., Ed.; Oxford University Press: New York, 1992; Vol. 2, pp 488−517.
(12) Yang, Y.; Denuault, G. *J. Chem. Soc., Faraday Trans.* **1996**, *92*, 3791–3798.
(13) Sánchez-Sánchez, C. M.; Rodríguez-López, J.; Bard, A. J. *Anal. Chem.* **2008**, *80*, 3254–3260.
(14) Unwin, P. R.; Bard, A. J. *Anal. Chem.* **1992**, *64*, 113–119.
(15) Unwin, P. R.; Bard, A. J. *J. Phys. Chem.* **1992**, *96*, 5035–5045.
(16) Selzer, Y.; Turyan, I.; Mandler, D. *J. Phys. Chem. B* **1999**, *103*, 1509–1517.
(17) Burt, D. P.; Cervera, J.; Mandler, D.; Macpherson, J. V.; Manzanares, J. A.; Unwin, P. R. *Phys. Chem. Chem. Phys.* **2005**, *7*, 2955–2964.
(18) Burshtain, D.; Mandler, D. *J. Electroanal. Chem.* **2005**, *581*, 310–319.
(19) Unwin, P. R.; Bard, A. J. *J. Phys. Chem.* **1991**, *95*, 7814–24.
(20) Zoski, C.; Luman, C. R.; Fernández, J. L.; Bard, A. J. *Anal. Chem.* **2007**, *79*, 4957–4966.
(21) Diaz-Ballote, L. F.; Alpuche-Aviles, M.; Wipf, D. O. *J. Electroanal. Chem.* **2007**, *604*, 17–25.
(22) Lie, L. H.; Mirkin, M. V.; Hakkarainen, S.; Houlton, A.; Horrocks, B. R. *J. Electroanal. Chem.* **2007**, *603*, 67–80.
(23) Slevin, C. J.; Unwin, P. R. *J. Am. Chem. Soc.* **2000**, *122*, 2597–2602.
(24) Mandler, D.; Unwin, P. R. *J. Phys. Chem. B* **2003**, *107*, 407–410.
(25) O'Mullane, A. P.; Macpherson, J. V.; Unwin, P. R.; Cervera-Montesinos, J.; Manzanares, J. A.; Frehill, F.; Vos, J. G. *J. Phys. Chem. B* **2004**, *108*, 7219–7227.
(26) Zhang, J.; Slevin, C. J.; Morton, C.; Scott, P.; Walton, D. J.; Unwin, P. R. *J. Phys. Chem. B* **2001**, *105*, 11120–11130.
(27) Liu, B.; Rotenberg, S. A.; Mirkin, M. V. *Anal. Chem.* **2002**, *74*, 6340–6348.
(28) Woods, R. Chemisorption at Electrodes. In *Electroanalytical Chemistry*; Bard, A. J., Ed.; Marcel Dekker: New York, 1976; pp 1−162.

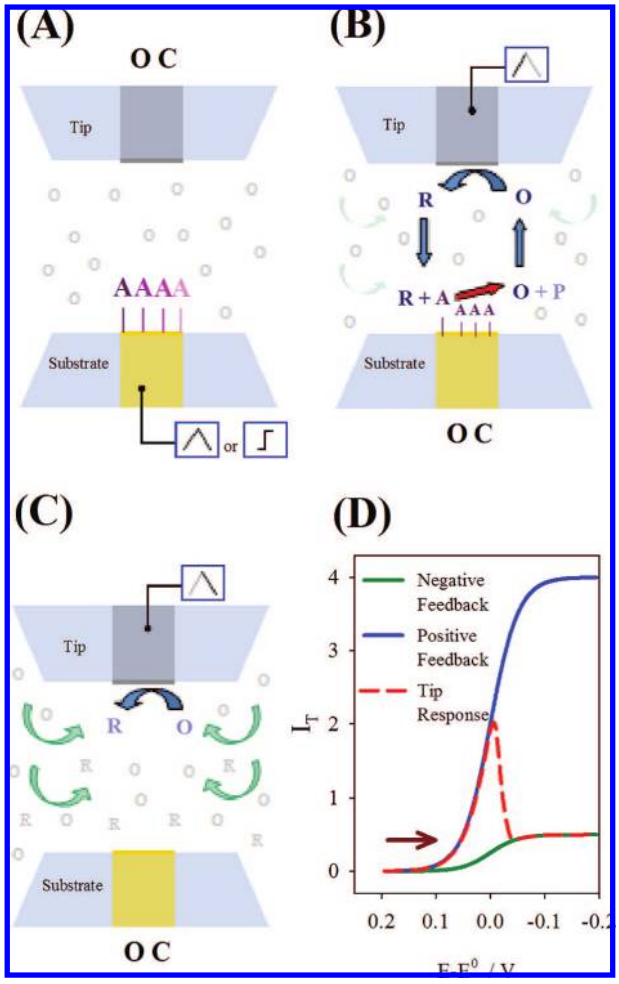

Figure 1. Schematics of the proposed mechanism for the surface interrogation. (A) A reactive species is chemically or electrochemically adsorbed at the substrate upon a potential scan or step while the tip is at open circuit. (B) The substrate is taken to open circuit, and the tip generates the titrant, which reacts at the surface of the substrate to support positive feedback at the same tip. (C) Upon consumption of the adsorbate at the substrate, the tip experiences negative feedback. (D) Expected current response at the tip following the events depicted in panels A−C for an arbitrary electrode setup.

transformed into a final product, P. Ideally, regeneration of O should only be possible through reaction with A present at the substrate, and the system would exhibit positive feedback only for as long as this condition is met. As shown in Figure 1C, the final state of the system is to show negative feedback, after all the A is depleted, and O reacts at the collector electrode at the rate governed by the hindered diffusion into the tip−substrate gap. Experimentally, this is difficult to achieve, and as discussed below, one requires a substrate with the same radius as that of the tip to have an acceptable working system.

Figure 1D shows the expected voltammetric response for this system (exaggerated for clarity) and compares it to the case of positive and negative feedback. The tip potential is scanned toward more negative potentials, and thus it is generating R, which diffuses to the substrate and reacts at its surface to regenerate O. Positive feedback persists as long as there is something to react at the substrate, and once the adsorbed species is consumed, the positive feedback drops and transforms into negative feedback. Notice that an important peculiarity in this experiment is that the SECM tip acts as both the titrant generator and detector, greatly simplifying the design of this in situ technique.

As depicted in Figure 1, the method assumes the use of a substrate electrode of the same shape and size as that of the SECM tip. There are a number of reasons for this choice, the most important being the presence of positive feedback at large unbiased electrodes[29−32] and the need to approach the SECM tip to very short distances. Positive feedback can occur in SECM, even if the substrate is under open-circuit conditions, when the substrate is larger than the UME disk of the SECM tip.[31] Previous SECM surface studies where this situation has been of experimental relevance[16,29] have used the configuration shown in this work. When the microdisks of the tip and substrate are of the same size and the substrate is allowed to rest at the open-circuit potential, it is possible to go from a complete negative feedback for very large values of the tip's RG, e.g., 10 (RG = r_g/a, where r_g is the radius of the insulating glass sheath), to a partial negative feedback for very small values of RG, e.g., 1.1. It is desirable to attain complete negative feedback, as this greatly improves the detection limits of the technique. However, as stated earlier, an adequate positive feedback is not present unless the distance between tip and substrate is very small, which is experimentally challenging when RG is large. A reasonable option is to establish larger values of positive feedback that greatly enhance the contrast with only partial negative feedback. In this case, both the tip and the substrate are the same size and shape, with an RG between 1 and 2. These tips, with $a = 12.5$ μm, can be approached to distances within 1 μm, at which positive feedback with $I_T = 6$ (or higher at smaller L-values) is typically attainable. Finally, different techniques can be used to generate the titrant, R; we have chosen to use CV, but the use of chronoamperometry is also shown and will be developed in future research.

Simulation

We performed digital simulations coupling voltammetry to the SECM geometry described in the previous section under transient conditions using the finite element method provided by the Comsol Multiphysics v.3.2 software (COMSOL, Inc., Burlington, MA). The simulation space is depicted in Figure 2, as discussed in the Simulation Model section, with further details in the Supporting Information. Basically, the problem was reduced to an axi-symmetric 2-D problem involving two equal size tips ($a = 12.5$ μm and RG = 1.5): the substrate tip with the adsorbed layer of interest and the tip, where reduction of the species O to R occurs. To treat the surface layer of A with the Multiphysics software, we use a very thin slab subdomain with a thickness of $d' < 0.01d$ in which the adsorbed species is confined. Since the gap between the tips was taken as $d = 1.25$ μm ($L = 0.1$), the adsorbed layer slab was taken as 10 nm. While this is thicker than an actual "surface layer" of adsorbate, the time required for diffusion of reactant, R, to cross this layer is so short (<1 μs) that this does not affect the results at the time scales of interest (especially considering any surface roughness of the substrate in an actual system).

Figure 3 shows representative results for the simulations at different values of the kinetic constant, k (for the reaction of

(29) Macpherson, J. V.; Slevin, C. J.; Unwin, P. R. *J. Chem. Soc., Faraday Trans.* **1996**, *92*, 3799–3805.
(30) Wipf, D. O.; Bard, A. J. *J. Electrochem. Soc.* **1991**, *138*, 469–474.
(31) Xiong, H.; Guo, J.; Amemiya, S. *Anal. Chem.* **2007**, *79*, 2735–2744.
(32) Zoski, C.; Simjee, N.; Guenat, O.; Koudelka-Hep, M. *Anal. Chem.* **2004**, *76*, 62–72.

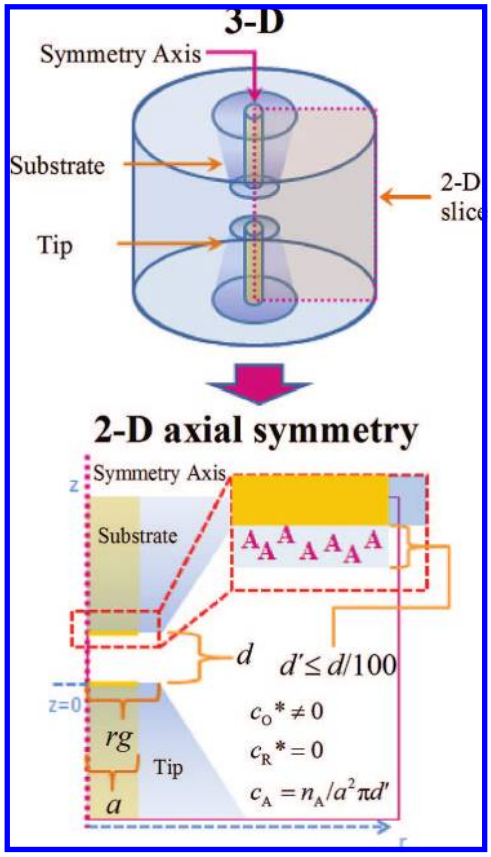

Figure 2. Schematics of the approach taken for digital simulations. For this study, $a = 12.5$ μm, $d = 1.25$ μm, $r_g = 18.75$ μm, $c_O = 1$ mol/m^3 (1 mM), and $d' = 0.01$ μm. Details of the simulation model are given in the Simulation Model section and in the Supporting Information. Substrate is above and SECM tip is below in this representation.

titrant R and A), and different amounts of adsorbed species A, represented as its charge, Q. In Figure 3A, the kinetic constant was varied over 3 orders of magnitude, and limiting behavior under these conditions is found when $k \geq 10^3$ m^3 mol^{-1} s^{-1} (mM^{-1} s^{-1}), as shown by the overlapping of the voltammograms with that of positive feedback before it reaches a maximum and decays as the surface is depleted of A. This limiting behavior establishes that the chemical reaction cannot regenerate O at a rate faster than the diffusion of R to the substrate; this is denoted as a titrant-limited situation. When k drops below this value, there is a shift in the peak, and the behavior is kinetically limited. Figure 3B shows the variation of the shape of the tip response with the simulated charge; i.e., the total amount of A was entered in the simulation under titrant-limited conditions ($k = 50$ m^3 mol^{-1} s^{-1}). The system responds proportionally to the amount of A following the positive feedback curve until A is depleted, when it rapidly drops to negative feedback behavior. Upon subtraction of the negative feedback curve to these tip responses and integration of the current with time, the collection efficiency (defined as the ratio of the charge recovered by the tip to the input charge used in the initial charging of the substrate) is found to be larger than 98%. This is another feature that can be achieved only at very small tip−substrate distances when using a substrate the same size as the tip, and it provides the advantage of obtaining the titrated charge by direct integration of the tip current without the need for using a calibration factor.

It is useful to have a titrant-limited system rather than a kinetically limited one. As shown in both panels in Figure 3, under titrant-limited conditions most of the collection takes place in a narrow potential region preceding the E^0 of the mediator and also exhibits very clear and distinguishable peaks (i.e., a larger contrast between positive and negative feedback). The advantage of the SECM technique compared to conventional CV is that it uncouples the generation of surface species from their detection and quantification. This allows one to detect species that would be difficult to see by CV. While the measurements described here were all made by scanning the tip through the entire mediator wave, it would also be possible to scan only through a portion of the wave and not attain a diffusion-limited plateau. This would be useful, for example, with a mediator whose reduction (or oxidation) occurs very close to the solvent background. Figure S1 in the Supporting Information shows some representative results of the simulations upon variation of the scan rate and through the use of chronoamperometry.

Experimental Section

All solutions were prepared with deionized Milli-Q water. Sulfuric acid (94−98%, Trace Metal grade), potassium nitrate, potassium chloride, zinc metal, tris(hydroxymethyl)aminomethane (TRIS, Molecular Biology grade), agar (Purified grade) and *o*-phosphoric acid (85%) from Fisher Scientific (Fair Lawn, NJ); silver nitrate (99+%,) silver wire (99.9%), and methyl viologen dichloride hydrate (98%) from Aldrich (Milwaukee, WI); dibasic potassium phosphate ("Baker Analyzed") from J.T. Baker (Phillipsbury, NJ); and hexaammineruthenium(III) chloride (99%, $Ru(NH_3)_6Cl_3$) from Strem Chemicals (Newburyport, MA) were used as received.

Gold (99.99+%) and platinum (99.99%) wires, 25 μm diameter, from Goodfellow (Devon, PA) were used to fabricate the SECM tips by procedures described elsewhere;[4] the tips used in this study had an RG ≤ 1.5. All electrodes were polished prior to use with alumina paste (0.05 μm) on microcloth pads (Buehler, Lake Bluff, IL), sonicated for 15 min in water, and cycled between 0 and 1 V versus NHE in 0.5 M sulfuric acid for 100 cycles to a constant CV. Phosphate buffer solution (PBS, pH 7) was prepared by adjusting the pH with *o*-phosphoric acid to a 0.3 M solution of dibasic potassium phosphate. TRIS buffer (pH 7) was prepared by adjusting the pH to a 0.3 M solution of TRIS base with sulfuric acid. Chloride-free solutions of hexaammineruthenium(III) were prepared by exchanging chloride for nitrate via potentiometric titration with 10 mM silver nitrate versus a Ag/AgCl working electrode; trace chloride was approximately 10 μM.

All solutions used in the electrochemical cell were bubbled with argon prior to the experiment and kept under a humidified argon blanket. A Ag/AgCl, saturated KCl reference electrode was used for all experiments. To avoid chloride contamination from leakage through the glass frit of the reference, a 1 M potassium nitrate−3% w/v agar gel salt bridge was used. All potentials in this study are referred to the NHE scale. In all experiments, the counter electrode was a piece of 0.5 mm tungsten wire from Alfa Products (Danvers, MA). The mediator concentration in all solutions used (either methyl viologen or hexaammineruthenium(III)) was 1 mM.

SECM and other electrochemical measurements were done in a CHI900 SECM station (CH Instruments, Austin, TX) with inchworm-based positioning. The electrode setup, as shown in Figures 1 and 2, was achieved by inserting the substrate from below a drilled Teflon electrochemical cell and positioning the SECM tip above it. The tip was scanned to locate electrochemically the center of the substrate electrode. It is critical to position the two UMEs concentrically, and we were able to achieve this within ±1 μm lateral error. The aligning procedure based on tip generation/substrate collection mode is described in detail in the Supporting Information.

Once the electrodes were positioned, their leads were connected to a three-way switch that allowed setting the working electrode

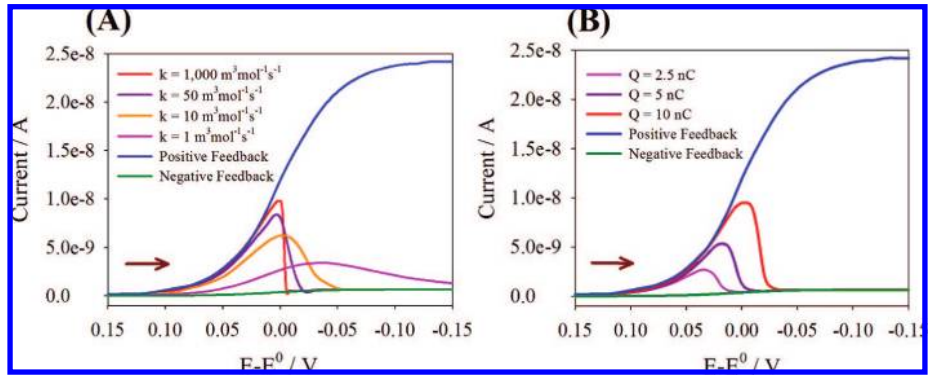

Figure 3. Representative results of digital simulations for the surface interrogation system showing linear sweep voltammograms for the first scan of the tip, $\nu = 50$ mV/s and $c_O = 1$ mol/m^3 (A) Variation of the reaction kinetic constant k at a fixed $Q = 8$ nC. (B) Variation of the charge adsorbed at the substrate Q at fixed $k = 50$ m^3 mol^{-1} s^{-1}.

lead in the SECM to the tip, to the substrate, or as a dummy; e.g., if the substrate was selected, the tip and the dummy were at open circuit. A typical measurement consisted of taking the substrate electrode to the desired potential through a linear scan at 50 mV/s and then turning off the cell at that potential, switching the working electrode lead to the tip, and turning on the cell with the programming for the tip scan. This scan was started at approximately 0.2 V versus the mediator E^0 (0.5 s quiet time to allow for double-layer charging) and run at 50 mV/s until −0.15 or −0.2 V versus E^0; the time delay between the end of the substrate scan and the beginning of the tip scan was typically 4 s. The tip was run for two complete cycles within these potential limits to verify the consumption of the adsorbed oxide and to obtain a blank for subtraction of negative feedback. The charge neutralized was calculated by numerical integration of the background- and baseline-subtracted voltammograms.

Independent quantification of the oxide was achieved with conventional CV on the substrates to validate the proposed SECM surface interrogation technique. In the case of Au, this process was investigated in situ in a scan prior to the oxidation of the substrate required to run the tip scans. In the case of Pt, separate measurements were required because of the accessible potential window.

Results and Discussion

To show the possibility of allowing a chemical reaction to maintain the positive feedback necessary for our measurements, we conducted preliminary experiments with the $Ru(NH_3)_6^{3+/2+}$ pair ($E^0 = 0.05$ V; in this study $E_{1/2} = 0.01$ V in PBS at pH 7 on either a Au or Pt electrode)[33] to evaluate the feasibility of the reduced form ($Ru(NH_3)_6^{2+}$) being able to reduce an electrogenerated oxide on a gold electrode. In its simplest scheme, we assume that the reaction (surface titration) in acid media proceeds as follows:

$$Au_2O_3 + 6Ru(NH_3)_6^{2+} + 6H^+ \rightarrow 2Au + 6Ru(NH_3)_6^{3+} + 3H_2O \quad (1)$$

where three electrons are transferred per gold atom. Based on the previous knowledge that the cyclic voltammogram of gold in PBS at pH 7 shows the onset of oxidation at approximately 0.9 V, the reaction with $Ru(NH_3)_6^{2+}$ is allowed thermodynamically ($\Delta E^0 \geq 0.85$). This is further confirmed in Figure 4A, where a gold tip was anodized to 1.2 V for 30 s; when the potential scan was reversed, a characteristic reduction wave was observed (green curve), but if an anodized electrode was immersed in a solution containing $Ru(NH_3)_6^{2+}$ (chemically generated from a 1 mM solution of $Ru(NH_3)_6^{3+}$ in PBS at pH 7 by passing through a Zn-packed syringe stored in an Ar-flushed vial) and returned to the electrochemical cell with a scan starting from the onset of the reduction wave, this oxide reduction process was not observed (blue curve). If the anodized electrode was instead immersed in a control solution of $Ru(NH_3)_6^{3+}$, the reduction wave was still present (red curve) with some losses that we attribute to some instability of the oxide upon changing environments.

As described in the Experimental Section, the relative positioning of the two electrodes is crucial to this experiment and is done first by means of the generation/collection mode, which is effective over longer distances, and then by positive feedback. Figure 4B shows a typical lateral scan for locating the center of the substrate electrode, in this case with the substrate producing $Ru(NH_3)_6^{2+}$ while the tip is oxidizing it back to $Ru(NH_3)_6^{3+}$; it is desirable to obtain symmetrical features in the current profiles of both electrodes. The inset in Figure 4C shows a typical approach curve once the centers of both electrodes have been found and the electrodes aligned. A good indicator for a successful alignment of the electrodes is the collapse of the substrate and tip currents to the same curve, which indicates nearly 100% collection efficiency (CE). Upon a potential scan as shown in the main Figure 4C, the same high CE should hold. Furthermore, obtaining such a scan confirms that the electrodes are not physically touching (short-circuited). The smoothly increasing current provided by the CV scan avoids problems with overloading the potentiostat that were frequently observed when a potential step was applied (chronoamperometry).

Once the electrodes are positioned well, the oxidation of the substrate and its subsequent interrogation can be performed. Figure 4D shows a typical result obtained from oxidation of a gold substrate at 1.4 V, followed by reduction by electrogenerated $Ru(NH_3)_6^{2+}$ with a positive feedback response in the tip. The general features expected from the simulation are present: the titration of the gold oxide by the reducing agent follows the curve of positive feedback until the consumption of all of the surface oxide causes a sharp decrease in the feedback current. Most of the charge neutralization occurs well before reaching $E_{1/2} = 0.01$ V, and after this, the current drops to the level of the expected negative feedback value ($I_T \approx 0.4$,[31] which for $i_{T,\infty} = 4$ nA gives $i_T = 1.6$ nA). A second cycle, without oxidation of the Au, shows that the initially present oxide has been consumed, as the clear peak observed during the first cycle

(33) Bard, A. J.; Fan, F.-R. F.; Mirkin, M. V. Scanning Electrochemical Microscopy. In *Electroanalytical Chemistry*; Bard, A. J., Ed.; Marcel Dekker: New York, 1994; pp 243−373.

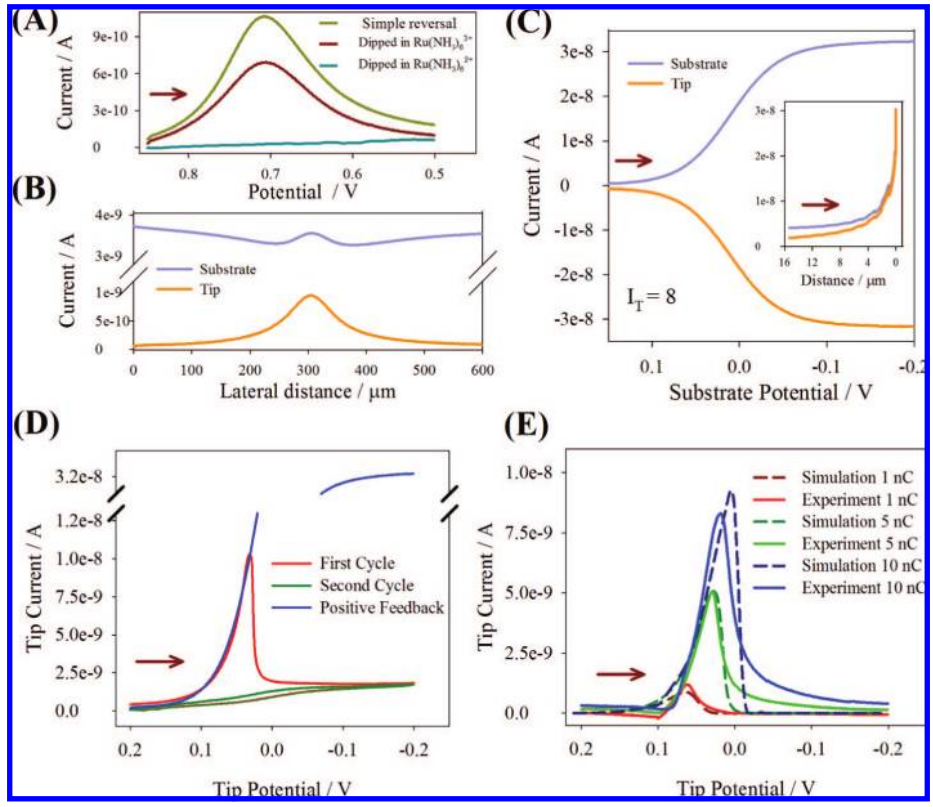

Figure 4. Experimental features of the technique. All potentials versus NHE. (A) A gold tip is oxidized for 30 s at 1.2 V in 0.3 M PBS, pH 7. The voltammograms correspond to the comparison of electroreduction just following oxidation (simple reversal, green curve) against the case when they are dipped in solutions containing either $Ru(NH_3)_6^{2+}$ (blue curve) or $Ru(NH_3)_6^{3+}$ (dark red curve), taken back to the cell, and the same scan run. Initial potential 0.85 V, $\nu = 50$ mV/s, dip time 2 s. (B) Line scan of the tip over the substrate, showing a desirable symmetry in the electrochemical response; the electrodes are centered at the correlated maxima of both curves. (C) Inset: Approach curve at the centered position in panel B, stopping at the highest current. The main curve shows a CV at this position in which the substrate is being scanned from 0.2 to −0.2 V and the tip is held at 0.2 V. (D) Representative result of the surface interrogation, showing the differences between the first and second cycles, $\nu = 50$ mV/s. The Au tip was oxidized for 30 s in 0.3 M TRIS buffer, pH 7, at 1.4 V. (E) Comparison between the simulated and experimental curves at different neutralized charges. The simulation used $k = 50$ m^3 mol^{-1} s^{-1}; experimental charges are within 10% of the simulated input for the surface oxide and correspond to the reduction of adsorbed oxygen on platinum.

does not appear. The second cycle voltammogram strongly resembles the one expected for negative feedback, although there is evidence that a very small amount of adsorbed oxygen is present even at these potentials, as is shown and discussed in the Supporting Information, Figure S2. For platinum oxide, the simplest chemical equations that can be written are for the reduction of the oxide obtained at high positive potentials, PtO_2, and for PtO, formed at lower potentials; eqs 2 and 3 hold for acidic conditions:

$$PtO_2 + 2Ru(NH_3)_6^{2+} + 2H^+ \rightarrow PtO + 2Ru(NH_3)_6^{3+} + H_2O \quad (2)$$

$$PtO + 2Ru(NH_3)_6^{2+} + 2H^+ \rightarrow Pt + 2Ru(NH_3)_6^{3+} + H_2O \quad (3)$$

These equations can be further separated into their elementary steps; however, as in the case of gold (eq 1), a discussion of the mechanism for the reduction process is beyond the scope of this study. Figure 4E presents a comparison of the experimental and simulated results for the case of platinum oxide that, as discussed later, exhibits only one peak in the collector scans. The comparison is based on the charge that is input in the simulation versus the amount calculated by integration in the experiment. The simulation fits quite well with the experiment, considering that the simulation takes into consideration only a simple single electron transfer process.

Minor differences between the experiment and the simulation may be caused by a slight misalignment of the electrodes, but more importantly, different reaction kinetics between the titrant and the different species and side reactions that may be involved in the electron transfer required to reach complete reduction of the oxide(s) to Pt. This is expected from the multiple number of electrons (i.e., mediator molecules) required for completion of the reaction. This may be the cause of the discrepancy between the sharp drops in current in the simulated curves versus the smooth drops observed in the experiment, which resembles the slower kinetic curves shown in Figure 3A. Such a discrepancy might also arise because of a coverage-dependent rate constant, which we do not take into account in the simulation model. Nonetheless, most of the charge neutralization is achieved under the titrant-limited regime, as discussed previously in the simulation model, which allows a straightforward quantification of the amount of oxide for both Pt and Au electrodes.

Figure 5 shows a comparison of results of the SECM surface interrogation and those conventionally obtained by the reduction of gold and platinum oxides by CV in PBS at pH 7 in the presence of 1 mM $Ru(NH_3)_6^{3+}$. Figure 5A shows the cyclic voltammograms of gold at selected reversal potentials; the amount of oxide is quantifiable above 1.0 V by integration of the surface reduction wave present between 0.8 and 0.5 V upon the cathodic scan. With CV, the oxidation of the substrate below

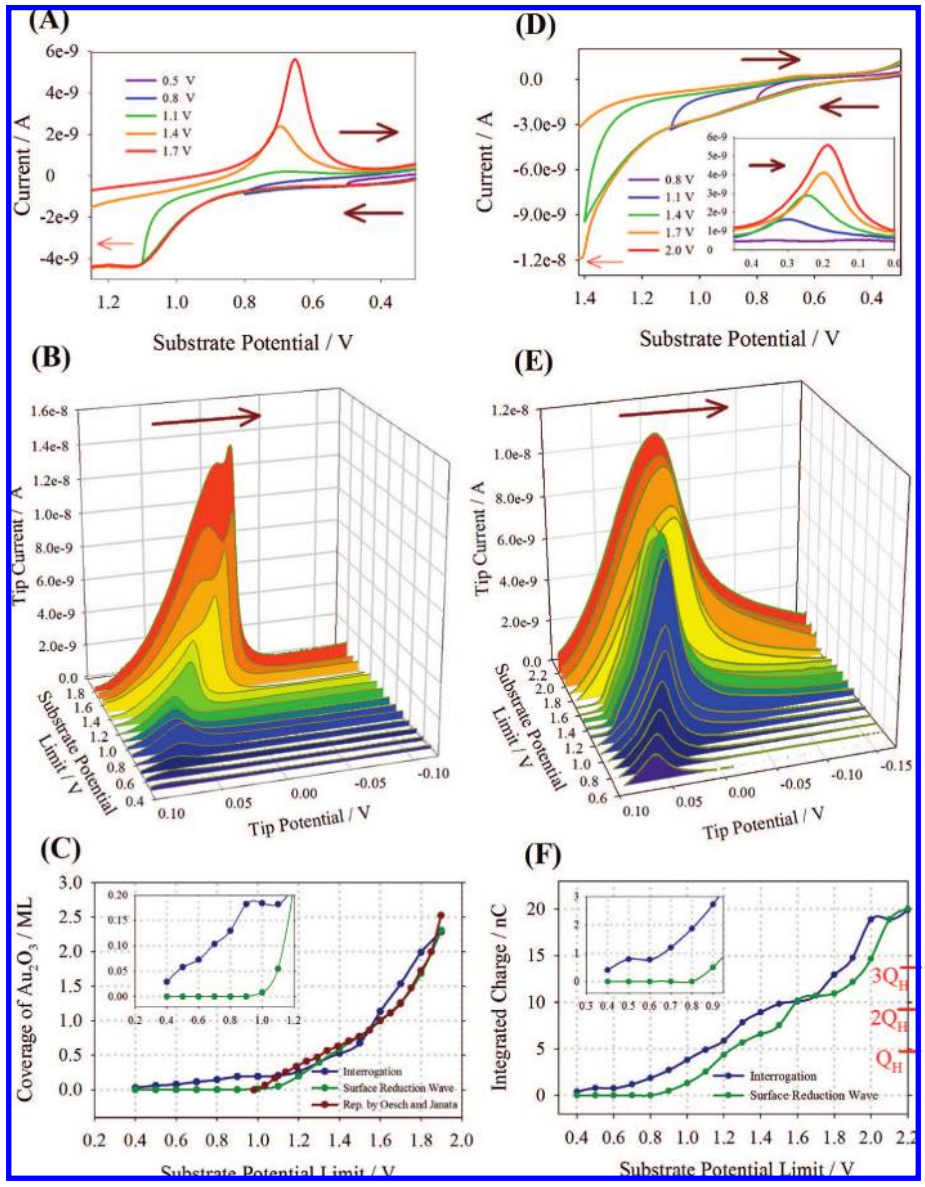

Figure 5. Results for the comparison of substrate voltammetry to the interrogation of Au (A−C) and Pt (D−F) in 0.3 M PBS, pH 7, with $Ru(NH_3)_6^{2+}$. All potentials versus NHE. (A) Voltammetry of the Au substrate, $\nu = 50$ mV/s, showing curves at different reverse potentials. (B) Spectrum of tip scans for the interrogation of Au electrodes taken to different potential limits, $\nu = 50$ mV/s. (C) Isotherm for oxygen on gold and comparison with ref 34. The inset shows a closeup in the low potential limit. (D,E) Same as (A) and (B) but for platinum. (F) Comparison of the integrated charge found with the interrogation technique versus the results of the electroreduction of the oxide in independent experiments. Q_H stands for the available electrochemical area of Pt, taken as the charge integration for the hydrogen adsorption peak.

0.9 V shows no presence of the surface reduction wave when reversing the scan, and presumably only double-layer charging. This is consistent with previous observations of gold oxidation in PBS at pH 7 reported by Oesch and Janata[34] and used as a reference for comparison in this study. Figure 5B shows the tip voltammograms obtained by the surface interrogation technique for increasingly positive potentials of the substrate. The feedback response shows three clearly defined regions in this set of curves. There is first a potential-dependent tip current signal that starts when the substrate is subjected to potentials well negative of 0.9 V and grows in at more positive potentials, finally stabilizing between 0.9 and 1.1 V. A following single peak then grows until $E_S = 1.4$ V, and finally a higher double-peaked signal appears for $E_S > 1.4$ V vs NHE. The total surface coverage on the substrate can then be obtained by integrating these tip reduction currents, and Figure 5C shows the isotherm for oxide coverage on the substrate versus E_S. The equivalent charge of a monolayer was obtained by the procedure suggested by Oesch and Janata[34] that consists in the measurement of the charge of the surface reduction wave before the onset of a second reduction of a species dubbed "oxide II" that appears between 0.4 and 0.2 V on the reverse scan and is taken to indicate the completion of two monolayers of Au_2O_3, independent of the roughness factor of the electrode. The comparison presented in Figure 5C shows very clearly that the SECM-based technique senses a reactive species adsorbed at less positive substrate potentials where the CV of the substrate electrode does not, in either results obtained here or those previously reported.[34] We believe this is evidence for the formation of the so-called "incipient oxide" or singly oxygenated species such as Au−OH

(34) Oesch, U.; Janata, J. *J. Electrochim. Acta* **1983**, *28*, 1237–1246.

or Au−O, which has recently been proposed to explain the catalytic activity toward CO oxidation present at noble metals at the liquid−solid[35−38] and gas−solid[39] interfaces. The coverage for the incipient oxide we observe is about 20% of a monolayer, which is consistent with very early observations done by capacitance measurements[40] (∼15%), electroreflection techniques[41] (10−20%), and more recent studies using contact electroresistance[42] (∼15%); indirect evidence is provided in photoelectrochemical[43] and SERS[44] studies by the enhanced adsorption of radioactively labeled alkaline earth cations[45] and by AC voltammetry.[46] An inherent feature of the surface interrogation technique is its ability to measure directly the charge that corresponds to such an adsorption feature, thus avoiding more complex treatments to estimate coverage. In considering the presence of these "incipient oxides", we must also take into account the possibility of titrating the accumulated positive charge in the double layer as a result of bringing the substrate to a potential more positive than the potential of zero charge (pzc). A simple calculation assuming a reasonably high value of the double-layer capacitance (30 μF/cm^2) and a roughness factor of 3, and reaching about 1 V difference from the pzc, yields a value of 0.4 nC for double-layer charging, which represents roughly 4% of the charge for a monolayer of gold oxide. This is just slightly higher than our limit of detection, as will be explained later, and while it may explain some effects observed at open circuit or at very low potentials (see the Supporting Information), it does not account for the amounts of incipient oxide found.

As previously noted, Figure 5B shows a transition between 1.4 and 1.5 V from a single-peaked tip response to a double-peaked one. From Figure 5C, this transition corresponds to the coverage reaching more than half of a monolayer. The finding of a change in behavior upon reaching discrete coverage values has been treated in the literature as an indicator of the presence or transformation of certain species.[47] However, in the present case it is difficult to discern between an actual surface behavior and an artifact from the reduction mechanism. As will be explained later, these features change with conditions such as the type of buffer. From a kinetic viewpoint, the second peak in the collector scans that appears at $E_S > 1.5$ V actually shows more facile kinetics for reaction with the reduced mediator than the first one, indicating that the first process is conditioned for its appearance; e.g., a sequential instead of a parallel mechanism for the reduction of two different oxide species would have to be invoked. This could involve, for example, a rearrangement of the oxygen moieties,[48] either spatially within the surface or chemically, e.g., the addition of a proton.[49]

Figure 5D−F shows a similar experiment with a platinum electrode in PBS at pH 7. The voltammograms that are obtained under these conditions are less reversible than those found in acid media,[47] and in fact, as shown in the inset of Figure 5D, the surface reduction wave is found in a region which overlaps the reduction of $Ru(NH_3)_6^{3+}$ ($E^0 = 0.05$ V). Thus, the direct measurement of platinum oxide reduction by CV had to be carried out in independent experiments in the absence of mediator. However, the SECM technique with mediator is especially useful in electrochemical measurements where certain surface processes are so irreversible that they are outside of the potential window of the working electrode or electrolyte and overlap with other waves. In such a case, direct electrochemical quantification is difficult. In the surface interrogation technique presented here, we can avoid this situation because the tip operates under different conditions than the substrate and can be made of a different material. Moreover, the electrochemical irreversibility is not an issue for this technique, since the positive feedback is maintained by a purely chemical reaction. For example, one might think that, because the surface reduction wave of platinum oxide and the reduction of $Ru(NH_3)_6^{3+}$ overlap, in the reaction of the platinum oxide with the titrant $Ru(NH_3)_6^{2+}$ the ΔG value would not be negative enough to cause the spontaneous reduction to occur. However, electrochemical irreversibility, as in the case of reduction of an oxide at large overpotentials, is a kinetic effect, not a thermodynamic one. Thus, the response of a platinum oxide to the titrant will be mostly a function of the difference in their redox potentials and will not be limited by the kinetics of the surface reduction of the oxide. Figure 5E shows the tip voltammogram spectrum for oxidized platinum; a clear difference from the spectrum of gold is the appearance of only one peak at all potentials that were studied but also that the rate of the titration reaction, Pt oxide with $Ru(NH_3)_6^{2+}$, appears to be more sluggish than found with Au, as inferred from the tailing of the peaks and the broader peaks for comparable charges. Just as in the case of Au, an analytical signal in the tip voltammograms is obtained below the potential limit at which the direct CV surface reduction shows up as appreciable current on the substrate voltammogram. Hence we assign this to an "incipient" oxide formation for the same reasons outlined previously for Au. Figure 5F shows this in more detail in the inset, a non-normalized isotherm. Unlike the case of Au, where a convenient strategy exists for normalizing the results, in the case of Pt traditionally the charge integrations have been divided by twice the charge integration for hydrogen adsorption (Q_H).[28] Because the hydrogen adsorption wave is less well defined in PBS buffer, the normalization procedure is less useful in PBS than it is in acidic media. An average value of 4.5 nC was found for Q_H for the Pt electrodes used based on measurements in acid media and can be used as a guideline. A comparison can be made between reported results and the isotherm shown in Figure 5F; it presents roughly an equivalence of one monolayer in the 1.1−1.2 V potential range based on Q_H[47] and an equivalent value of approximately 2.3 for $Q/2Q_H$ in the potential range above 2 V, although not a very clear stabilization to a limiting value is seen.[28] Clearly, however,

(35) Hayden, B. E.; Rendall, M. E.; South, O. *J. Am. Chem. Soc.* **2003**, *125*, 7738–7742.
(36) Beltramo, G. L.; Shubina, T. E.; Koper, M. T. M. *Chem. Phys. Chem.* **2005**, *6*, 2597–2606.
(37) Spendelow, J. S.; Goodpaster, J. D.; Kenis, P. J. A.; Wieckowski, A. *J. Phys. Chem. B* **2006**, *110*, 9545–9555.
(38) Assiongbon, K. A.; Roy, D. *Surf. Sci.* **2005**, *594*, 99–119.
(39) Kim, T. S.; Gong, J.; Ojifinni, R. A.; White, J. M.; Mullins, C. B. *J. Am. Chem. Soc.* **2006**, *128*, 6282–6283.
(40) Schmid, G. M.; O'Brien, R. N. *J. Electrochem. Soc.* **1964**, *11*, 832–837.
(41) Nguyen Van Huong, C.; Hinnen, C.; Lecoeur, J. *J. Electroanal. Chem.* **1980**, *106*, 185–191.
(42) Marichev, V. A.; Russ, J. *Electrochem* **1999**, *35*, 434–440.
(43) Watanabe, T.; Gerischer, J. *J. Electroanal. Chem.* **1981**, *117*, 185–200.
(44) DeSilvestro, J.; Weaver, M. J. *J. Electroanal. Chem.* **1986**, *209*, 377–386.
(45) Horányi, G. *Electrochim. Acta* **1991**, *36*, 1453–1463.
(46) Lertanantawong, B.; O'Mullane, A. P.; Surareungchai, W.; Somasundrum, M.; Burke, L. D.; Bond, A. M. *Langmuir* **2008**, *24*, 2856–2868.
(47) Conway, B. E.; Angerstein-Kozlowska, H. *Acc. Chem. Res.* **1981**, *14*, 49–56.
(48) Angerstein-Kozlowska, H.; Conway, B. E.; Barnett, B.; Mozota, J. *J. Electroanal. Chem.* **1979**, *100*, 417–446.
(49) Pletcher, D.; Sotiropoulos, S. *J. Chem. Soc., Faraday Trans.* **1994**, *90*, 3663–3668.

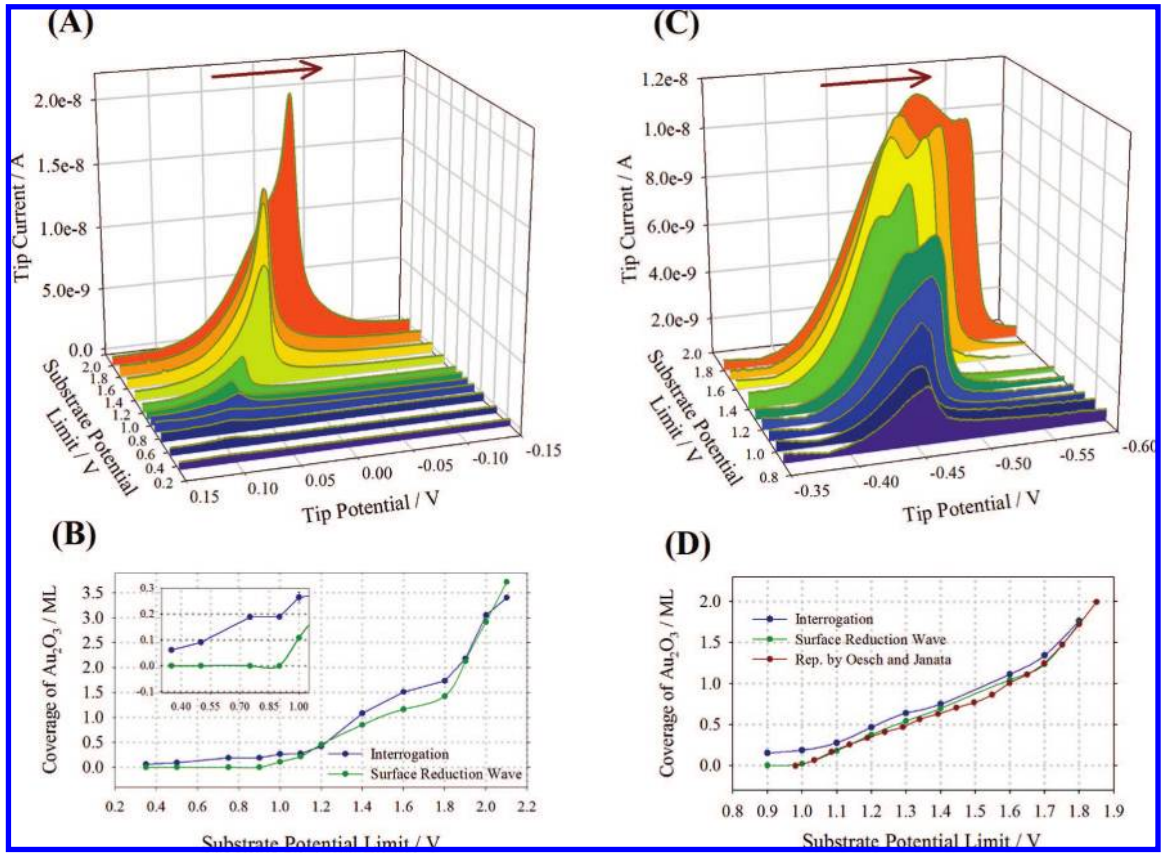

Figure 6. Interrogation of gold electrodes under different conditions. All potentials versus NHE. (A) Spectrum of tip scans in 0.3 M TRIS buffer, pH 7, holding the substrate at the indicated potential for 30 s, $\nu = 50$ mV/s. (B) Isotherm for the conditions in (A). The insert shows a closeup in the low potential limit. (C) Spectrum of tip scans in 0.3 M PBS, pH 7, using the MV^{2+}/MV^{+} mediator pair, $\nu = 50$ mV/s. (D) Isotherm for the conditions in (C) and comparison to ref 34.

the behaviors of both the surface reduction wave and the surface interrogation plots correlate. Upon reaching the range 1.6−1.7 V, both curves exhibit a plateau ($\sim 2Q_H$) that continues with further growth of the oxide; above these limits, the raw curves from the surface interrogation show an increased background which interferes with a clean integration of the voltammograms, most likely because of suitable conditions for the production of large amounts of oxygen coming from water oxidation or even platinum dissolution.[28]

The nature of the solution ions can affect the behavior of the oxide films. Figure 6 shows the results of the surface interrogation to gold oxidation when TRIS buffer is used in place of PBS. Figure 6A displays the behavior of gold oxide (generated by holding the electrode for 30 s at the desired potential) in TRIS buffer; unlike PBS at pH 7, which contains the $HPO_4^{2-}/H_2PO_4^{-}$ pair which is negatively charged, TRIS contains the $(CH_2OH)_3CNH_2/(CH_2OH)_3CNH_3^{+}$ pair which is positively charged, and in this case, SO_4^{2-} is used as a counterion. Changing the nature of the buffer will affect adsorption at the positive polarization required for anodization of the gold substrate, so that TRIS would be less likely to interact with the electrode. The spectrum of tip voltammograms shown in Figure 6A contrasts clearly with the one shown in Figure 5B, as it exhibits only one peak at low and moderate polarizations. From the isotherm in Figure 6B, one can assign the appearance of the shoulder in the tip scans at high polarizations to the formation of the so-called "oxide II" which occurs after completion of two monolayers and whose onset is the basis of the isotherm normalization for gold.[34] Despite the differences in the shape of the collector response with PBS and TRIS buffer, the results in Figures 6B and 5C are similar. Note that near 1.8 V the isotherm reaches a limiting coverage of 2 monolayers, and that the shape of this response corresponds very well to that exhibited by the surface reduction wave. At low potentials, a limiting value of 0.2 monolayer is reached at about 1.0 V, even when the system is allowed to remain for a longer time at this potential. This further supports our assumption that this feature corresponds to the "incipient oxide".

We also show in Figure 6 results obtained with another redox mediator to support the independence of the surface characterization response on mediator used. We selected the methyl viologen pair $MV^{2+/+}$ ($E^0 = -0.44$ V, experimental $E_{1/2} = -0.46$ V),[50] whose reduced form is a stronger reducing agent than $Ru(NH_3)_6^{2+}$. Figure 6C presents the tip scans for interrogation of gold oxide in PBS at pH 7, and Figure 6D the corresponding isotherm which shows good agreement with the literature reference results[34] and with the CV surface reduction wave, although compared to Figure 5B ($Ru(NH_3)_6^{2+}$ titrant), a slight excess charge is found at all potentials. This might be the result of an increased reactivity toward a subsequent oxide with the MV^{+} species or, more likely, to its increased sensitivity to the presence of oxygen (either electrogenerated by water oxidation or present residually during the experiment). As with $Ru(NH_3)_6^{3+/2+}$, the presence of two processes in the tip scans is observed with $MV^{2+/+}$, although they are slightly different in shape and proportions than the ones observed with

(50) Fultz, M. L.; Durst, R. A. *Anal. Chim. Acta* **1982**, *140*, 1–18.

$Ru(NH_3)_6^{2+}$. These results indicate that, although the mechanism of the surface reduction may be different with different mediators, the quantification of Au_2O_3 is similar (cf. Figures 5C and 6D), indicating complete detection of submonolayer amounts of the oxide.

In the work described, we chose CV to obtain the tip response. The use of chronoamperometry would perhaps be more desirable for routine quantification, and we have also explored this approach (Figure S3 in the Supporting Information). CV provided us with diagnostic features of the voltammograms, reproducible results, and good figures of merit; in the case of gold our estimated limit of detection (taken as 3 times the average standard deviation of our measurements) is 0.24 nC, which for the roughness factors found in our gold electrodes (typically between 2 and 3) represents 2.1−3.4% of a monolayer. This figure is also equivalent to 49 $\mu C/cm^2$ of geometric area (16−25 $\mu C/cm^2$ of real area considering the above-mentioned roughness factors). Furthermore, because of the overlapping between the positive feedback scans and the tip response, we were able to verify experimental aspects such as the alignment of the electrodes. Chronoamperometry does not allow such straightforward diagnostics, and we found it to be less reproducible; however, these results are preliminary and its final implementation is yet to be undertaken.

Conclusions

A new electrochemical in situ technique to study surfaces based on the transient feedback mode of SECM for the quantification of adsorbed species at electrodes has been described. Here an electrogenerated titrant reacts with the electrogenerated adsorbate at the substrate electrode at open circuit and generates a positive feedback response at the SECM tip only while the adsorbate is present. The technique is analogous to a directed redox titration, and because of its SECM feedback characteristics, the experimental setup is simplified by having a SECM tip behave as both titrant generator and detector. Its operation was verified through the study of stable electrogenerated oxide species on the surface of Au and Pt. The experimental results are in general agreement with the known behavior of these systems and with the results from digital simulations, thus confirming the proposed mode of operation.

Isotherms for the coverage of oxygen species with potential on Au and Pt are presented at neutral pH. The results obtained by the proposed SECM surface interrogation agree on a first level very well with those previously reported and obtained by conventional CV of the substrate. However, they provide deeper insight into the formation of species that may, in fact, be at too small a level or obscured by other processes occurring during a conventional potential scan on a substrate. For example, our results strongly suggest the formation of "incipient oxides" on Au and Pt at less positive potentials that are detected by virtue of the sensitivity of the titration of the substrate surface and that are not observed on the cathodic part of the substrate CV. This feature offers the advantage of detecting species at the potential at which they are formed by means of a chemical reaction and not at the potential at which they become electrochemically detectable. The detection of the gold oxides was tested with two different titrants, $Ru(NH_3)_6^{2+}$ and MV^+, thus confirming the operation principle. While there were small differences in the reduction mechanisms as observed in the collector responses, the quantification in both cases was very similar. Changing other conditions, such as the buffer composition, also influenced the shape of the response; however, the correspondence to the expected behavior remained. This new analytical tool should be useful for the study of adsorption phenomena at electrocatalysts and in the characterization of surface modified materials, and studies in this area are under way.

Simulation Model

The total simulation space consists of two relevant subdomains: the first one corresponds to the usual SECM setup for two UMEs (a substrate and a tip, both with $a = 12.5$ μm and RG = 1.5) that are being approached, and the second one represents the thin slab described previously. The gap between the tips is set to 1.25 μm, which implies $L = 0.1$. In the first subdomain, we consider only a diffusion problem in which the reduced species R is being generated at the tip from the initially present oxidized species O. Thus, for transient conditions following Fick's second law as required for implementing linear voltammetry, we have eqs 4 and 5:

$$\frac{\partial c_O}{\partial t} = D_O \nabla^2 c_O \tag{4}$$

$$\frac{\partial c_R}{\partial t} = D_R \nabla^2 c_R \tag{5}$$

where c_O and c_R are the concentrations of oxidized and reduced species, respectively, and are functions of r, z, and time t. D_O and D_R are the diffusion coefficients of these species and are given the value of 5.5×10^{-10} m^2/s, which corresponds to the $Ru(NH_3)_6^{3+}$ cation.[51] The bulk concentration of species is set to the one used during the experiment, $c_O^* = 1$ mol/m^3 and $c_R^* = 0$ mol/m^3 (1 mol/m^3 = 1 mM); the adsorbed species A is not present in this subdomain. At the tip boundary, $z = 0$, $0 < r < a$, we write the inward flux condition following Butler−Volmer kinetics, eqs 6 and 7, and the linear potential sweep in eq 8:

$$-D_O \nabla c_O = -k^\circ e^{-\alpha f(E-E^0)} c_O(0,r) + k^\circ e^{(1-\alpha) f(E-E^0)} c_R(0,r) \tag{6}$$

$$-D_R \nabla c_R = k^\circ e^{-\alpha f(E-E^0)} c_O(0,r) - k^\circ e^{(1-\alpha) f(E-E^0)} c_R(0,r) \tag{7}$$

$$E = E_{in} - \nu t \tag{8}$$

where k° is the heterogeneous rate constant, chosen to be 0.1 m/s, avoiding thus any kinetic complication, α the symmetry factor equal to 0.5; f, which is equal to 38.94 V^{-1} at 298 K, and E^0 the standard potential of the reaction. E is the potential and relates the scan to time t by means of the scan rate ν, which is set to 0.05 V/s, and the initial potential E_{in}. The second subdomain consists of the thin slab in which the adsorbed species A is contained and the reduction reaction shown in eq 9 occurs; its thickness was set to 0.01 μm.

$$R + A \xrightarrow{k} O \tag{9}$$

This element is considered to be permeable for both O and R, and their diffusion coefficients remain the same as in the first subdomain. The adsorbed species A, however, is not mobile in the thin slab; this is a reasonable assumption, as any surface diffusivity is irrelevant to the dimensions of the substrate and assumed to be negligible in the time scale of the experiment. Because of this, eqs 10 and 11 for O and R contain both diffusive and kinetic components, while eq 12 is a purely kinetic

(51) Baur, J. E.; Wightman, R. M. *J. Electroanal. Chem. Int. Electrochem.* **1991**, *305*, 73–81.

function. The kinetic component is assumed to be a second-order process associated with a kinetic constant k.

$$\frac{\partial c_O}{\partial t} = D_O \nabla^2 c_O + k c_R c_A \quad (10)$$

$$\frac{\partial c_R}{\partial t} = D_R \nabla^2 c_R - k c_R c_A \quad (11)$$

$$\frac{\partial c_A}{\partial t} = -k c_R c_A \quad (12)$$

Because this thin slab is a two-dimensional representation of a three-dimensional object, just as the rest of the elements in the simulation, it is now possible to specify the amount of adsorbate in terms of a concentration. This concentration is calculated as the number of moles n_A of adsorbed species divided by the volume element represented by the whole thin slab, as shown in Figure 2. While for the simulation it is necessary to calculate n_A, it is much easier to refer to this quantity in terms of the charge it carries; thus, the charge Q is equal to n_A times Faraday's constant $F = 96\,485$ C/mol. A convenient way to normalize the results obtained through the approximation used above in terms of a more widely used quantity as the surface coverage Γ_A is provided in the Supporting Information.

The current read at the tip is obtained by integrating the normal diffusive flux of the oxidized species at its surface and multiplying by a geometric argument to solve for the geometry, as shown in eq 13. In all simulations we assume a one-electron transfer, $n = 1$, for both R to A and O to R.

$$i_{tip} = \int_{r=0}^{r=a} 2\pi n F D_O r \frac{\partial c_O(r,0)}{\partial z}\, dr \quad (13)$$

Acknowledgment. The support of this research by the National Science Foundation (CHE 0451494) and the Robert A. Welch Foundation (F-0021) is gratefully acknowledged. J.R.-L. thanks Secretaría de Educación Pública of México for a SEP-DGRI scholarship support.

Supporting Information Available: Digital simulations coupling cyclic voltammetry to the SECM geometry under transient conditions using the finite element method. This material is available free of charge via the Internet at http://pubs.acs.org.

JA8050553